Refractive Index Seen by a Probe Beam Interacting with a Laser-Plasma System

D. Turnbull,* C. Goyon, G. E. Kemp, B. B. Pollock, D. Mariscal, L. Divol, J. S. Ross, S. Patankar, J. D. Moody, and P. Michel
Lawrence Livermore National Laboratory, Livermore, California 94550, USA
(Received 5 October 2016; published 5 January 2017)

We report the first complete set of measurements of a laser-plasma optical system's refractive index, as seen by a second probe laser beam, as a function of the relative wavelength shift between the two laser beams. Both the imaginary and real refractive index components are found to be in good agreement with linear theory using plasma parameters measured by optical Thomson scattering and interferometry; the former is in contrast to previous work and has implications for crossed-beam energy transfer in indirect-drive inertial confinement fusion, and the latter is measured for the first time. The data include the first demonstration of a laser-plasma polarizer with 85%–87% extinction for the particular laser and plasma parameters used in this experiment, complementing the existing suite of high-power, tunable, and ultrafast plasma-based photonic devices.

DOI: 10.1103/PhysRevLett.118.015001

There has been a recent surge of interest in using laser-plasma optical systems to manipulate the basic properties of light waves [1–4]. Plasma-based photonic devices are attractive because they can be ultrafast, damage resistant, and easily tunable. Alleviating optic damage concerns by replacing conventional optics with plasma-based components could enable the next generation of high-power, large-scale laser facilities. Plasma gratings in particular have received a great deal of attention because they are routinely used to mediate crossed-beam energy transfer (CBET) in indirect-drive inertial confinement fusion (ICF) experiments at the National Ignition Facility (NIF) [5–7]. Numerous "inline" CBET models that all rely on the same linear theory have been incorporated into radiation-hydrodynamic codes [8–10]. However, multiple experiments [11,12]—including ICF experiments at the NIF [13,14]—have consistently failed to observe the level of energy transfer expected on the basis of linear theory, raising questions regarding the theory's validity.

In indirect-drive ICF, CBET calculation errors could introduce time-dependent radiation flux asymmetries in the hohlraum drive—a primary source of yield degradation in targets fielded with a high initial gas fill [15]. Recent targets have lowered the initial gas fill in large part to reduce CBET and other laser-plasma instabilities, but these targets rapidly fill with wall material such that symmetry control remains a key challenge, and furthermore, the range of available design options is severely constricted [16–19]. In direct-drive ICF, CBET reduces the implosion hydrodynamic efficiency, and its mitigation is considered essential for demonstrating performance improvements [20–22]. In both cases, validating linear crossed-beam energy transfer theory with direct measurements is a first step toward demonstrating its controllability and expanding the operable parameter space for integrated ICF experiments.

Recently, that theory was revisited when it was recognized that plasma gratings could also be used to dynamically control the polarization of light waves [1,23]. The effect of a laser-plasma system on a second laser beam probing the system can be described by a complex refractive index perturbation that is a function of the wavelength shift between the interacting beams; the system can thus (anisotropically) modify both the phase and the amplitude of the probe and therefore act as a wave plate and/or a polarizer [1]. Several teams have now demonstrated polarization changes induced when using degenerate (same frequency) beams, which isolates the impact on phase [2,24]. In this Letter, we report the use of wavelength tuning to more fully map out the complete refractive index perturbation in the vicinity of the ion acoustic resonance. The real component is measured as a function of the wavelength shift for the first time and is observed to disappear at the ion acoustic resonance, as predicted. The imaginary component, which underlies crossed-beam energy transfer experiments in both direct- and indirect-drive ICF, is measured with sufficient accuracy to resolve both nonresonant and resonant energy transfer and is found to be in excellent agreement with linear theory (both for the first time). The data also include the first demonstration of a laser-plasma polarizer with 85%–87% extinction, further complementing the existing suite of plasma-based photonic devices.

Our optical system consists of a plasma and a "pump" laser beam with electric field E_0 and frequency ω_0. A probe laser beam with E_1 and ω_1 will encounter resonances if $\omega_1 - \omega_0 = \pm\omega_{iaw}$; i.e., the frequency difference between the two beams is equal to the frequency of an ion acoustic wave with wave number $k_b = |\boldsymbol{k}_0 - \boldsymbol{k}_1|$. The driven ion acoustic wave mediates energy transfer between the two beams, thus modifying the probe's amplitude. As described

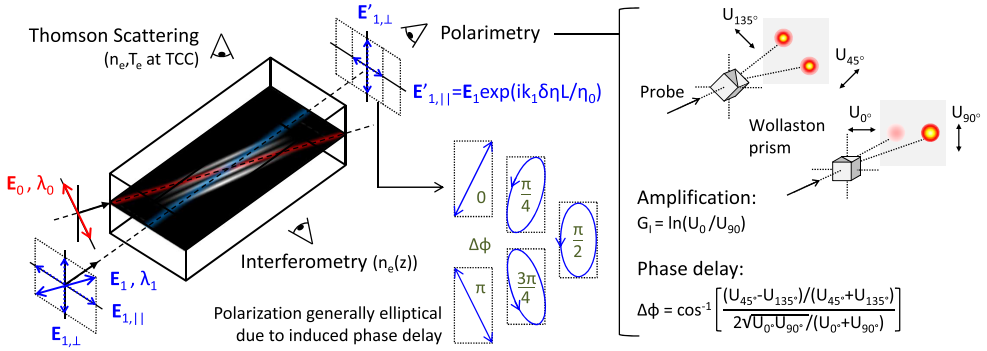

FIG. 1. The presence of the pump introduces anisotropy to the plasma as seen by a probe beam. Only the component of the probe's polarization that is aligned with the pump polarization will have its amplitude and/or phase modified by the interaction, both of which can be measured using polarimetry.

by the Kramers-Kronig relations, any frequency-dependent variation of the probe's amplitude in the vicinity of an optical resonance must be accompanied by variation in the real refractive index seen by the probe. The net impact of the pump on the probe beam can be described as a complex refractive index perturbation $\delta\eta$ such that $E_1' = E_1 \exp(ik_1\delta\eta L/\eta_0)$ after interacting with the laser-plasma system, where L is the interaction length and η_0 is the unperturbed plasma refractive index. The full expression for the refractive index perturbation was derived by Michel *et al.* [1] using a kinetic plasma model. Critically, the perturbation is only seen by the component of the probe's electric field that is parallel to the projection of the pump's electric field in the probe's plane of polarization (c.f. Fig. 1) [1,23]. The ability to induce anisotropy via the relative orientation of the pump and probe polarizations can be exploited for precise manipulation of the probe's polarization [2].

The experiment was conducted at Lawrence Livermore National Laboratory's Jupiter Laser Facility. A gas jet equipped with a 3 mm outlet diameter supersonic nozzle released methane gas prior to the arrival of the pump and probe, which were focused over the nozzle with a relative crossing angle of 27°. Two different phase plates were used to give the pump and probe speckled but roughly flattop (in an average sense) intensity distributions with 600 and 200 μm diameters at best focus, respectively. The pump had a $\approx$3 ns square pulse shape and established the plasma conditions prior to the arrival of the probe, which had a $\approx$250 ps Gaussian pulse shape with the peak delayed $\approx$1.3 ns from the rise of the pump. Using the nominal pump energies (292 ± 8 J), fast diode-based pulse shape measurements, and an assumed spot size based on the phase plate properties, the pump intensity was expected to be in the range of $I_0 = (3.6 \pm 0.2) \times 10^{13}$ W/cm^2 averaged over the interaction region. The initial probe energy and intensity were $\approx$27 mJ and 3.4×10^{11} W/cm^2, respectively. Both beams used the fundamental frequency of a Nd:YLF laser ($\lambda \approx 1053$ nm), but different front ends allowed wavelength tuning within the bandwidth of the gain medium; here, a range of $-3 \leq \Delta\lambda \leq +3$ Å was used, where $\Delta\lambda$ is the wavelength difference between pump and probe. A polarizer was used before the last turning mirror to orient the probe polarization close to 45° relative to the horizontal pump polarization. This provides a convenient and novel method of diagnosing probe amplitude changes induced by the laser-plasma system; exploiting the anisotropic nature of the interaction, only the horizontal component of the probe's polarization will either grow or decay under the influence of the pump, and the orthogonal vertical polarization provides a baseline that factors in shot-to-shot variation of the incident probe beam energy as well as inverse bremsstrahlung absorption in the plasma, as shown in Fig. 1. Separating the polarizations with a Wollaston prism subsequent to the interaction and taking their ratio provides a direct measure of the amplification. To compare with linear theory, the plasma electron density and temperature were measured with Thomson scattering. The scattered light was dominated by the high-energy pump beam, collected at a scattering angle of 90°, and directed to a streaked spectrometer measuring the blueshifted electron plasma wave feature. For additional information about density gradients in the plasma, optical interferometry was used, employing a dedicated diagnostic beam that was incident on the plasma orthogonal to the pump beam. Both diagnostics were analyzed at the time of the pump-probe interaction. The experimental setup is shown in Fig. 1.

The effect of the refractive index perturbation's imaginary component can be expressed as a gain exponent G, where $E_{1,\|}' = E_1 \exp(G)$ and $G = -k_1 \mathrm{Im}[\delta\eta] L/\eta_0$. Intensity being proportional to the square of the electric field, the intensity gain exponent is $G_I = 2G$ and is related to amplification, the ratio of intensity in each polarization subsequent to the interaction, by $G_I = \ln(A)$. Therefore, the imaginary component of the refractive index perturbation can be inferred from the amplification. Figure 2 shows the experimental data plotted with a calculation using the linear theory developed to compute crossed-beam energy transfer in indirect-drive ICF

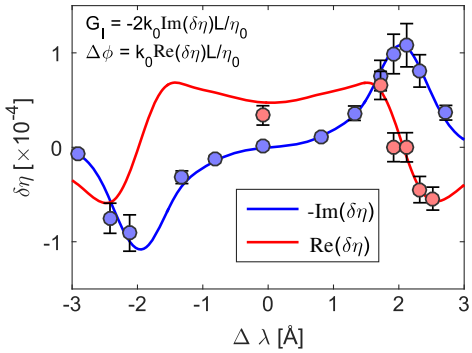

FIG. 2. The real (red) and imaginary (blue) refractive index perturbation components are plotted as a function of the wavelength shift between the pump and probe. Experimental measurements (points) are plotted along with the linear theory (solid lines) used to calculate CBET at the NIF. The parameters used in the linear theory calculation are listed in the text and are quite consistent with measured values (where available) and three-dimensional HYDRA simulations.

experiments at the NIF [5]. The electron density and temperature inputs used in the calculation were $n_e/n_c = 0.0104$ and $T_e = 220$ eV, where n_c is the critical density, consistent with the experimentally measured values of $n_e/n_c = 0.011 \pm 0.001$ and $T_e = 224 \pm 24$ eV. Since several necessary inputs were not directly measured, three-dimensional radiation-hydrodynamic simulations using HYDRA [25] were performed in order to obtain estimates for ion temperature and flow velocity. The pump beam energy, spatial profile, and pulse shape used in the simulation closely reproduced the experimental conditions, and the initial methane gas density and the flux limiter were then adjusted in order to match the measured electron density and temperature. The simulations predicted an ion temperature of $T_i/T_e \approx 0.09$, whereas $T_i/T_e = 0.115$ is used in the linear theory best fit. The difference is small and is comparable to the level of ion heating expected from thermalizing the energy in the driven ion acoustic waves, which is not included in the simulations. HYDRA also predicts an outwardly directed radial flow resulting from the expansion of the plasma channel formed by the pump beam, which broadens the ion acoustic resonance by shifting the peak in different portions of the interaction region; this was directly imported into the linear theory calculation due to the lack of a flow velocity measurement. The effective pump intensity was also reduced 20% from the expected value (to $I_0 = 2.9 \times 10^{13}$ W/cm^2), which we attribute to unmeasured transport losses through the final optics, inverse bremsstrahlung absorption in the plasma, pump depletion effects, and/or imperfect focusing of the pump beam. In specifying the crossing angle, the calculation takes into account refraction as well as the finite spread given by the $f/6.7$ and $f/10$ pump and probe beams, respectively, which also broadens the ion acoustic resonance. Finally, the resonance peak location was most easily matched by specifying the ion species fractions as $f_C = 0.3$ and $f_H = 0.7$, whereas $f_C = 0.2$ and $f_H = 0.8$ were expected based on the initial methane gas composition. This implies that species separation is occurring in this system. In principle, hydrogen—being lighter and having a higher charge-to-mass ratio—is expected to lead the plasma channel expansion, leaving a higher concentration of carbon in the interaction region. This effect has been observed previously using simultaneous electron and ion feature Thomson scattering in an expanding CH plasma [26,27]. However, assessing this quantitatively requires multi-ion-fluid simulations and is considered outside the scope of this study. Species separation is an increasingly active field of research in the ICF community [28–32].

It is evident that the linear theory accurately reproduces the data both near the resonance peaks as well as in the off-resonant region between the Stokes and anti-Stokes peaks. Previous work utilizing a simple geometry had determined that crossed-beam energy transfer was maximized near the ion acoustic resonance, but the peak location was not predicted accurately, the data lacked the precision to measure off-resonant transfer, and it was determined that the gain was lower than expected from linear theory by a factor of 20 [11]. In ICF hohlraums, there has also been evidence that the amount of energy transfer is less than expected from linear theory [13,14]. In both previous examples, the linear theory calculations used plasma conditions taken entirely from radiation-hydrodynamic simulations. The agreement found in this better-characterized experiment suggests that inaccuracies in the assumed density and temperature may be one source of discrepancy. Weak turbulence effects associated with having many of these coupled-beam interactions in the same region of plasma may also be a factor in indirect-drive ICF [13]. Note that, while the conditions of this experiment are very different from an ICF environment in terms of wavelength, intensity, density, and temperature, it can still be considered a good surrogate by several metrics. Gain was larger in this experiment than even the most resonant of interactions in an ICF hohlraum, so this can be considered an upper bound on the parameter space relevant to ICF. Furthermore, the normalized ion acoustic wave damping is $\nu/\omega_{iaw} \approx 0.1$–$0.2$ (i.e., strongly damped) in both cases; achieving this in the present experiment motivated the use of the multispecies methane gas [33].

As mentioned, the imaginary refractive index perturbation component is accompanied by a real refractive index change, which introduces a phase delay between the probe's vertical (noninteracting) and horizontal (interacting) components. While amplification was determined by separating the vertical and horizontal components and taking their ratio (which is insensitive to the phase delay), inferring the phase delay $\Delta\phi$ requires a second measurement in which the Wollaston prism is rotated 45° in order to separate the 45° and 135° polarization components. With each signal's energy in arbitrary units given by U_j,

where j is the polarization angle, the phase delay for each pair of measurements (assuming polarized light and perfect shot-to-shot reproducibility) is given by

$$\Delta\phi = \cos^{-1}\left(\frac{(U_{45^\circ} - U_{135^\circ})/(U_{45^\circ} + U_{135^\circ})}{2\sqrt{U_{0^\circ}U_{90^\circ}}/(U_{0^\circ} + U_{90^\circ})}\right). \quad (1)$$

Unlike the imaginary component, the real component of the refractive index perturbation is nonzero even in the absence of a wavelength shift between the pump and probe [23]. Turnbull *et al.* exploited this property previously to convert an initially elliptical polarization into a nearly ideal circular polarization [2]. Here, wavelength tuning capability allows us to validate other points along the real refractive index perturbation curve, as is also shown in Fig. 2. Again, the linear theory provides a good match to the experimental data using the same parameters that were used to fit the amplification data, with key features—nonzero phase delay at zero wavelength shift, larger dephasing on either side of the resonance, and zero dephasing at the peak—evident in the data. Note that the measurement does not actually discriminate between positive and negative phase delay, but since the data are consistent with the shape of the curve as predicted by linear theory, we assume that those points to the left of the peak are positive and points to the right of the peak are negative. This is the first (to our knowledge) measurement of a laser-plasma optical system's real refractive index perturbation as a function of wavelength tuning.

The experiment was designed in such a way to test the concept of a "plasma polarizer," which was proposed by Michel *et al.* [1]. When $\lambda_1 - \lambda_0 < 0$, the probe transfers energy to the pump but only out of its horizontal component (which is aligned with the pump polarization) due to the anisotropy of the laser-plasma system, so the system is effectively a linear polarizer. The data point at the negative peak of Fig. 2 represents an extinction of 85%. The data themselves are shown in Fig. 3; the incident polarization was oriented in order to have nearly equal horizontal and vertical components, but after propagating through the system the horizontal polarization is significantly attenuated. Additional shots were conducted in which the incident probe intensity was increased up to $I_1 \approx 3 \times 10^{12}$ W/cm^2, and the extinction stayed in the range of 85%–87%. Note that the probe is otherwise minimally affected by the system because the phase delay induced between the vertical polarization and what is left of the horizontal polarization is close to zero near the resonance peak, absorption in this fairly tenuous plasma is calculated to be modest, and the probe is not degraded by other laser-plasma instabilities. Maintaining similar plasma conditions, the extinction could be increased or decreased by changing the pump intensity. This demonstrates another ultrafast, damage-resistant, and tunable laser-plasma photonic device.

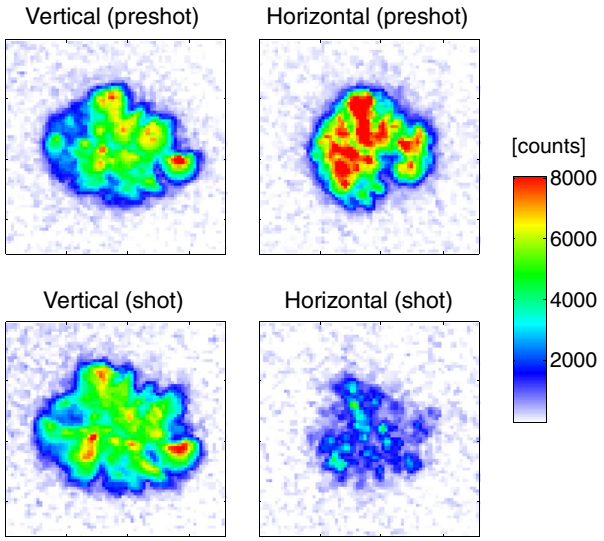

FIG. 3. The anisotropic laser-plasma system acts like a pure linear polarizer at the negative resonance peak, depleting the probe's horizontal polarization component. The color scale for each pair is normalized to the vertical polarization. The vertical and horizontal spots appear different because the Wollaston prism slightly affects the imaging. The preshot images are obtained without any plasma, and the horizontal polarization is brighter than the vertical polarization because the polarizer setting the incident polarization was not quite oriented at 45°; 85%–87% of it is then extinguished by the laser-plasma polarizer, whereas the vertical polarization is minimally perturbed by the system.

Having now achieved both a wave plate and a polarizer, it is possible to design a laser Q switch using only laser-plasma systems.

In summary, a laser-plasma optical system's complete refractive index perturbation—both its imaginary and real components—was measured as a function of wavelength shift in the vicinity of the ion acoustic resonance for the first time. It was found to be in excellent agreement with the linear theory that is used to compute crossed-beam energy transfer in indirect-drive ICF experiments. The ability to correctly predict energy transfer in this well-characterized context, but not in ICF experiments [13,14], points to possible errors in the hydrodynamic inputs to the ICF calculations and/or weak turbulence effects from having many such coupled-beam interactions in the same volume of plasma. Polarization is shown to be an effective diagnostic of CBET, which is in turn sensitive to numerous laser and plasma parameters; here it revealed species separation during the plasma evolution as likely playing a role in the interaction. We also achieved the first demonstration of a laser-plasma polarizer, which extinguished 85%–87% of a probe beam's horizontal polarization.

This work was performed under the auspices of the U.S. Department of Energy by Lawrence Livermore National Laboratory under Contract No. DE-AC52-07NA27344. This work was supported by the LLNL-LDRD Program under Project No. 42074. We thank the staff of the Jupiter

Laser Facility and Suzanne Ali for enabling a successful experimental campaign. D. T. also acknowledges useful discussions regarding species separation with C. Bellei, P. Amendt, and G. Kagan.

*turnbull@lle.rochester.edu
Present address: University of Rochester Laboratory for Laser Energetics, 250 E River Rd., Rochester, New York 14623, USA.

[1] P. Michel, L. Divol, D. Turnbull, and J. D. Moody, Phys. Rev. Lett. **113**, 205001 (2014).
[2] D. Turnbull, P. Michel, T. Chapman, E. Tubman, B. B. Pollock, C. Y. Chen, C. Goyon, J. S. Ross, L. Divol, N. Woolsey, and J. D. Moody, Phys. Rev. Lett. **116**, 205001 (2016).
[3] D. J. Stark, C. Bhattacharjee, A. V. Arefiev, T. Toncian, R. D. Hazeltine, and S. M. Mahajan, Phys. Rev. Lett. **115**, 025002 (2015).
[4] G. Lehmann and K. H. Spatschek, Phys. Rev. Lett. **116**, 225002 (2016).
[5] P. Michel, L. Divol, E. A. Williams, S. Weber, C. A. Thomas, D. A. Callahan, S. W. Haan, J. D. Salmonson, S. Dixit, D. E. Hinkel, M. J. Edwards, B. J. MacGowan, J. D. Lindl, S. H. Glenzer, and L. J. Suter, Phys. Rev. Lett. **102**, 025004 (2009).
[6] S. H. Glenzer *et al.*, Science **327**, 1228 (2010).
[7] J. D. Moody *et al.*, Nat. Phys. **8**, 344 (2012).
[8] I. V. Igumenshchev, D. H. Edgell, V. N. Goncharov, J. A. Delettrez, A. V. Maximov, J. F. Myatt, W. Seka, A. Shvydky, S. Skupsky, and C. Stoeckl, Phys. Plasmas **17**, 122708 (2010).
[9] A. Colaïtis, G. Duchateau, X. Ribeyre, and V. Tikhonchuk, Phys. Rev. E **91**, 013102 (2015).
[10] D. J. Y. Marion, A. Debayle, P.-E. Masson-Laborde, P. Loiseau, and M. Casanova, Phys. Plasmas **23**, 052705 (2016).
[11] R. K. Kirkwood, B. B. Afeyan, W. L. Kruer, B. J. MacGowan, J. D. Moody, D. S. Montgomery, D. M. Pennington, T. L. Weiland, and S. C. Wilks, Phys. Rev. Lett. **76**, 2065 (1996).
[12] R. K. Kirkwood, J. D. Moody, A. B. Langdon, B. I. Cohen, E. A. Williams, M. R. Dorr, J. A. Hittinger, R. Berger, P. E. Young, L. J. Suter, L. Divol, S. H. Glenzer, O. L. Landen, and W. Seka, Phys. Rev. Lett. **89**, 215003 (2002).
[13] P. Michel, W. Rozmus, E. A. Williams, L. Divol, R. L. Berger, R. P. J. Town, S. H. Glenzer, and D. A. Callahan, Phys. Rev. Lett. **109**, 195004 (2012).
[14] R. P. J. Town *et al.*, Phys. Plasmas **18**, 056302 (2011).
[15] D. S. Clark, C. R. Weber, J. L. Milovich, J. D. Salmonson, A. L. Kritcher, S. W. Haan, B. A. Hammel, D. E. Hinkel, O. A. Hurricane, O. S. Jones, M. M. Marinak, P. K. Patel, H. F. Robey, S. M. Sepke, and M. J. Edwards, Phys. Plasmas **23**, 056302 (2016).
[16] N. B. Meezan *et al.*, Plasma Phys. Controlled Fusion **59**, 014021 (2017).
[17] D. Turnbull, P. Michel, J. E. Ralph, L. Divol, J. S. Ross, L. F. Berzak Hopkins, A. L. Kritcher, D. E. Hinkel, and J. D. Moody, Phys. Rev. Lett. **114**, 125001 (2015).
[18] D. Turnbull, L. F. Berzak Hopkins, S. Le Pape, L. Divol, N. Meezan, O. L. Landen, D. D. Ho, A. Mackinnon, A. B. Zylstra, H. G. Rinderknecht, H. Sio, R. D. Petrasso, J. S. Ross, S. Khan, A. Pak, E. L. Dewald, D. A. Callahan, O. Hurricane, W. W. Hsing, and M. J. Edwards, Phys. Plasmas **23**, 052710 (2016).
[19] S. Le Pape *et al.*, Phys. Plasmas **23**, 056311 (2016).
[20] I. V. Igumenshchev *et al.*, Phys. Plasmas **19**, 056314 (2012).
[21] V. N. Goncharov *et al.*, Phys. Plasmas **21**, 056315 (2014).
[22] S. P. Regan *et al.*, Phys. Rev. Lett. **117**, 025001 (2016).
[23] J. K. Wahlstrand and H. M. Milchberg, Opt. Lett. **36**, 3822 (2011).
[24] J. H. Odhner, D. A. Romanov, E. T. McCole, J. K. Wahlstrand, H. M. Milchberg, and R. J. Levis, Phys. Rev. Lett. **109**, 065003 (2012).
[25] M. M. Marinak, G. D. Kerbel, N. A. Gentile, O. Jones, D. Munro, S. Pollaine, T. R. Dittrich, and S. W. Haan, Phys. Plasmas **8**, 2275 (2001).
[26] J. S. Ross, H.-S. Park, P. Amendt, L. Divol, N. L. Kugland, W. Rozmus, and S. H. Glenzer, Rev. Sci. Instrum. **83**, 10E323 (2012).
[27] P. Amendt, C. Bellei, J. S. Ross, and J. Salmonson, Phys. Rev. E **91**, 023103 (2015).
[28] J. R. Rygg, J. A. Frenje, C. K. Li, F. H. Sguin, R. D. Petrasso, J. A. Delettrez, V. Y. Glebov, V. N. Goncharov, D. D. Meyerhofer, S. P. Regan, T. C. Sangster, and C. Stoeckl, Phys. Plasmas **13**, 052702 (2006).
[29] G. Kagan and X.-Z. Tang, Phys. Plasmas **19**, 082709 (2012).
[30] C. Bellei and P. A. Amendt, Phys. Rev. E **90**, 013101 (2014).
[31] M. J. Rosenberg *et al.*, Phys. Plasmas **21**, 122712 (2014).
[32] H. G. Rinderknecht, M. J. Rosenberg, C. K. Li, N. M. Hoffman, G. Kagan, A. B. Zylstra, H. Sio, J. A. Frenje, M. Gatu Johnson, F. H. Séguin, R. D. Petrasso, P. Amendt, C. Bellei, S. Wilks, J. Delettrez, V. Y. Glebov, C. Stoeckl, T. C. Sangster, D. D. Meyerhofer, and A. Nikroo, Phys. Rev. Lett. **114**, 025001 (2015).
[33] E. A. Williams, R. L. Berger, R. P. Drake, A. M. Rubenchik, B. S. Bauer, D. D. Meyerhofer, A. C. Gaeris, and T. W. Johnston, Phys. Plasmas **2**, 129 (1995).